

Preparation and preliminary biological evaluation of a ^{177}Lu labeled sanazole derivative for possible use in targeting tumor hypoxia

Tapas Das,^a Sudipta Chakraborty,^a Sharmila Banerjee,^{a,*} Archana Mukherjee,^a Grace Samuel,^a H. D. Sarma,^b C. K. K. Nair,^b V. T. Kagiya^c and Meera Venkatesh^a

^aRadiopharmaceuticals Division, Bhabha Atomic Research Centre, Mumbai 400085, India

^bRadiation Biology and Health Sciences Division, Bhabha Atomic Research Centre, Mumbai 400085, India

^cHealth Research Foundation, Yoshida Kawara-cho 14, Kyoto 606, Japan

Received 9 July 2004; revised 6 September 2004; accepted 8 September 2004

Available online 2 October 2004

Abstract—The preparation of a polyazamacrocyclic-nitrotriazole conjugate for radiolabeling with the therapeutic radioisotope viz. ^{177}Lu is described. The nitroimidazole used for the present study is [N-2'-(carboxyethyl)-2-(3'-nitro-1'-triazolyl)acetamide], the carboxylic acid derivative of sanazole, which possesses an optimal combination of desired properties such as, selective toxicity for hypoxic cells, lowered lipophilicity resulting in lowered neurotoxicity. The bifunctional chelating agent is a DOTA derivative viz. 1,4,7,10-tetraaza-1-(4'-aminobenzylacetamido)-cyclododecane-4,7,10-triacetic acid (*p*-amino-DOTA-anilide). ^{177}Lu was produced in adequate specific activity (110 TBq/g) and high radionuclidic purity (~100%) by irradiating enriched (60.6% ^{176}Lu) Lu_2O_3 target and used for radiolabeling of the sanazole-BFCA conjugate. ~98% Complexation yield was achieved under optimized conditions. The complex has been characterized by paper chromatography and HPLC studies. Bioevaluation studies in Swiss mice bearing fibrosarcoma tumors revealed moderate tumor uptake (0.88%/g at 1 h post-injection) with favorable tumor to blood (4.00 at 1 h post-injection) and tumor to muscle (4.63 at 1 h post-injection) ratios.

© 2004 Elsevier Ltd. All rights reserved.

1. Introduction

In connection with an ongoing project on development of new agents for imaging hypoxia with radioisotopically labeled compounds, we have used metronidazole, a readily available 5-nitroimidazole as the hypoxia-avid substrate.¹ A combination of an ideal redox potential along with an optimum lipophilicity are the contributing factors toward the choice of the ideal nitroimidazole for targeting hypoxia.^{2,3} In this respect, it has been documented that metronidazole possesses a reduction potential of -415mV , which while efficiently reduces it in anaerobes, renders it ineffective under aerobic conditions.^{3,4} In order to achieve a more versatile nitroimidazole, which could exhibit wider applicability, the position of substitution of the nitro group in the nitroimidazole was varied leading to the development of the 2-nitroim-

idazoles such as, misonidazole.⁵ Misonidazole exhibits three useful properties in hypoxic cells, such as, sensitization to ionizing radiation, direct cytotoxicity, and covalent binding.^{5,6} However, in achieving the desirable redox potential, the increased lipophilicity of the compounds led to undesirable side-effects such as, enhancement of neurotoxicity.⁷ This issue could be addressed in two different approaches. While in one, development of a new agent, which would possess a higher radiosensitizing ability translating to lower clinical doses and therefore reduction in the toxicity levels could be envisaged, the other constitutes modification of the existing 2- or 5-nitroimidazoles to yield a compound with lower lipophilicity and hence lower toxicity.^{8,9} Subsequent efforts to tailor molecules with the desired properties have led to the development of [N-2'-(methoxyethyl)-2-(3'-nitro-1'-triazolyl)acetamide] or sanazole, which exhibits selective toxicity for hypoxic cells, lowered lipophilicity and hence, lower neurotoxicity.^{10,11} Since our current interest was toward designing an agent for radiotherapy of tumor hypoxia, wherein therapeutic doses

Keywords: Hypoxia; Targeted tumor therapy; Sanazole; ^{177}Lu .

* Corresponding author. Tel.: +91 22 2559 2449; fax: +91 22 2550 5345; e-mail: sharmila@apsara.barc.ernet.in

of the radiolabeled agent needs to be administered, sanazole was an obvious choice.

In our earlier attempts, wherein the targeted agent was intended for use toward diagnostic detection and imaging of hypoxia, the isotope of obvious choice was ^{99m}Tc .¹ In recent times, ^{177}Lu with its ideal nuclear characteristics [$T_{1/2} = 6.71$ d, $E_{\beta(\text{max})} = 497$ keV, $E_{\gamma} = 208$ keV (11%), 113 keV (6.4%)] has been identified as the radioisotope of choice for therapeutic use in radiopharmaceutical preparations.^{12–15} It could be produced in excellent radiochemical and radionuclidic purity with adequate specific activity using moderate flux reactors owing to the very high thermal neutron capture cross-section ($\sigma = 2100$ b) of ^{176}Lu .^{12,16} Since direct radiolabeling of the sanazole derivative chosen in the present study is difficult to achieve, indirect incorporation of ^{177}Lu through suitable bifunctional chelating agent (BFCA) is envisaged. A careful survey of literature indicates that polyazamacrocycles are ideal BFCA for complexation with lanthanides.¹⁷ The advantages provided by macrocycles such as, 1,4,7,10-tetraazacyclododecane-1,4,7,10-tetraacetic acid (DOTA) or its derivatives in forming thermodynamically stable complexes with ^{177}Lu coupled with its high kinetic inertness, which constitutes a desirable feature for in vivo usage provide impetus to the choice of suitable DOTA derivative as the BFCA in the present study.^{17,18} The sanazole derivative available with us being [N-2'-(carboxyethyl)-2-(3'-nitro-1'-triazolyl)acetamide] (I), the carboxylic acid derivative of sanazole, the DOTA derivative chosen to effect the desired conjugation was 1,4,7,10-tetraaza-1-(4'-aminobenzylacetamido)-cyclododecane-4,7,10-triacetic acid (*p*-amino-DOTA-anilide, II). In the present paper, we report our findings toward the development of a ^{177}Lu labeled sanazole derivative-*p*-amino-DOTA-anilide conjugate (III) as a targeted agent for hypoxic tissues. To the best of our knowledge, this paper constitutes the first of its kind in reporting the possible use of a potential agent for radiotherapy of tumor hypoxia.

2. Results and discussion

2.1. Characterization of the sanazole derivative-*p*-amino-DOTA-anilide conjugate (III)

The conjugate (III) was characterized by using spectroscopic techniques such as, FT-IR and ^1H NMR spectroscopy. The data obtained are reported below.

FT-IR (KBr, ν cm^{-1}): 3443, 3096, 2966, 2853, 1682, 1631, 1555; ^1H NMR (CD_3OD , δ ppm): 3.40–3.78 (16H, m, cyclic CH_2), 4.11–4.24 (6H, m, N(DOTA)- $\text{CH}_2\text{-COOH}$), 4.30–4.38 (2H, m, N(DOTA)- $\text{CH}_2\text{-CO-NH}$), 4.76 (2H, dd, $J = 2.2$ and 14.3 Hz, sanazole-N- $\text{CH}_2\text{-CO}$), 5.11 (4H, dd, $J = 9.9$ and 23 Hz, -CO- $\text{CH}_2\text{-CH}_2\text{-CO}$), 8.07 (2H, br s, CONH-aromatic H), 8.09 (1H, s, sanazole H), 8.11–8.13 (2H, m, CONH-aromatic H).

The peak multiplicities and integrations observed in the high resolution ^1H NMR spectrum of the sanazole

derivative-*p*-amino-DOTA-anilide conjugate (III) was consistent with the structure of the expected compound. Appearance of the peaks at δ 5.11 and 4.76 corresponding to the protons of the sanazole moiety indicate the desired conjugation. The deshielded proton of the triazole ring of sanazole observable at δ 8.09 provides further evidences toward the desired derivatization.

2.2. Production of ^{177}Lu

$\sim 3 \times 10^3$ Ci/g (110 TBq/g) of ^{177}Lu activity was obtained at 6 h post end of bombardment (EOB) when 60.6% enriched Lu_2O_3 target was irradiated at a thermal neutron flux of 3×10^{13} n/cm²/s for 7 d. The radionuclidic purity of ^{177}Lu produced was $\sim 100\%$ as estimated by analyzing the γ ray spectrum. A typical γ ray spectrum of ^{177}Lu after radiochemical processing is shown in Figure 1. The major γ peaks observed were 72, 113, 208, 250 and 321 keV, all of which correspond to the photopeaks of ^{177}Lu .¹⁶ This was further confirmed from the decay of counts per second values at those peaks according to the half-life of ^{177}Lu .

It is well documented that there is a possibility of formation of ^{177m}Lu ($T_{1/2} = 160.5$ d) on thermal neutron bombardment of Lu_2O_3 target.^{19,20} However, γ ray spectrum of the irradiated Lu target after chemical processing did not show any significant peak corresponding to the photopeaks of ^{177m}Lu (128, 153, 228, 378, 414, 418 keV).¹⁶ This is expected as the radioactivity due to ^{177m}Lu produced will be insignificant and below the detectable limit on a 7 d irradiation owing to its long half-life and comparatively low cross-section ($\sigma = 7$ b) of its formation. Assay of trace level of ^{177m}Lu activity present in ^{177}Lu activity produced was carried out by recording γ ray spectrum of a sample aliquot, initially having high radioactive concentration, after complete decay of ^{177}Lu activity (45–65 d EOB). The average level of radionuclidic impurity burden in ^{177}Lu due to ^{177m}Lu was found to be 150 nCi of ^{177m}Lu /1 mCi of ^{177}Lu (5.5 kBq/37 MBq) at EOB.

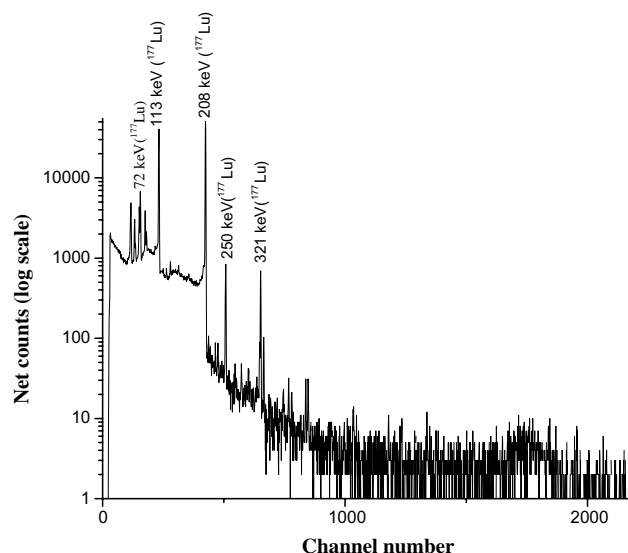


Figure 1. A typical γ ray spectrum of ^{177}Lu .

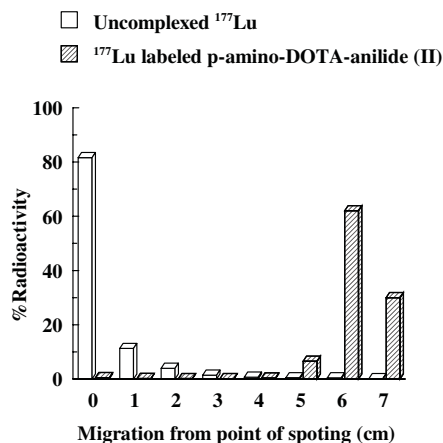


Figure 2. Paper chromatography patterns of the ^{177}Lu labeled *p*-amino-DOTA-anilide (II) and uncomplexed ^{177}Lu using normal saline as eluting solvent.

2.3. Characterization of the ^{177}Lu labeled *p*-amino-DOTA-anilide (II)

The characterization of the ^{177}Lu labeled *p*-amino-DOTA-anilide (II) was carried out by paper chromatography using normal saline as the eluting solvent. It was observed that the radiolabeled BFCA moved toward the solvent front ($R_f = 0.8\text{--}1$) while the uncomplexed ^{177}Lu remained almost at the point of spotting ($R_f = 0\text{--}0.1$) under identical conditions. The paper chromatography patterns of the ^{177}Lu labeled *p*-amino-DOTA-anilide and uncomplexed ^{177}Lu are shown in Figure 2. The extent of complexation as determined from the paper chromatography studies was $>99\%$ when $50\mu\text{g}$ of the BFCA was used and the reaction was carried out for 15 min at room temperature at pH 5.

2.4. Characterization of the ^{177}Lu labeled sanazole derivative-*p*-amino-DOTA-anilide conjugate (III)

The ^{177}Lu labeled conjugate was characterized and its radiochemical purity was determined by paper chromatography using 50% aqueous acetonitrile as the eluting solvent. It was observed that in this chromatography system, both uncomplexed ^{177}Lu as well as ^{177}Lu labeled BFCA (II) did not show any migration from the point of spotting ($R_f = 0$), while ^{177}Lu labeled conjugate (III) exhibited $R_f = 0.5\text{--}0.75$. The paper chromatography patterns of uncomplexed ^{177}Lu , ^{177}Lu labeled BFCA, and ^{177}Lu labeled conjugate are shown in Figure 3.

2.5. Optimization of the complexation yield of ^{177}Lu labeled sanazole derivative-*p*-amino-DOTA-anilide conjugate (III)

In order to optimize the reaction conditions for obtaining maximum radiolabeling yield, several experiments were carried out varying the reaction parameters such as, ligand concentration, incubation time, and temperature.

In a $200\mu\text{L}$ reaction volume ligand (III) concentration was varied from 10 to $200\mu\text{g}$. It was observed that while

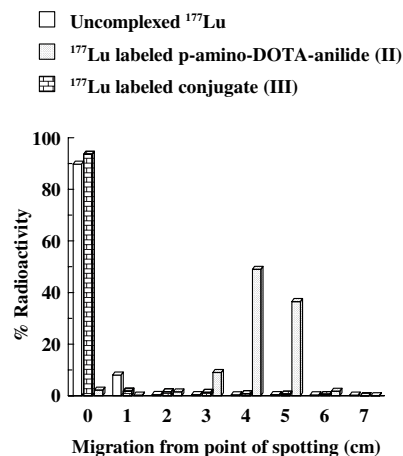


Figure 3. Paper chromatography patterns of uncomplexed ^{177}Lu , ^{177}Lu labeled *p*-amino-DOTA-anilide (II), and ^{177}Lu labeled sanazole derivative-*p*-amino-DOTA-anilide conjugate (III) using 50% aqueous acetonitrile as the eluting solvent.

only 12.4% radiolabeling yield was achieved using $10\mu\text{g}$ ligand, it increased to 97.8% with $100\mu\text{g}$ of ligand. Further increase in ligand concentration did not show any appreciable effect on the labeling yield. Variation of radiolabeling yield of the ^{177}Lu labeled conjugate with ligand concentration is shown in Figure 4.

It is well reported that ^{177}Lu labeling of biomolecules are mostly carried out below pH 7.^{21,22} In the present case, maximum complexation was obtained when the reaction was carried out in 0.1 M ammonium acetate buffer maintaining the pH of the reaction mixture ~ 5 .

To study the effect of temperature on reaction kinetics, the complexation was carried out by incubating the reaction mixture both at room temperature as well as at 50°C and the complexation yields were determined at different time intervals in both the cases. While maximum complexation yield of 88.5% was obtained at room temperature after 1 h of incubation, 97.8% complexation was achievable within 30 min when the reaction mixture was incubated at 50°C . The effect of incubation time and temperature on the complexation yield of the ^{177}Lu labeled conjugate (III) is depicted in Figure 5.

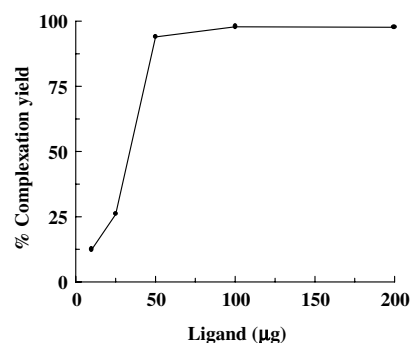


Figure 4. Effect of variation of ligand concentration on the complexation yield of ^{177}Lu labeled sanazole derivative-*p*-amino-DOTA-anilide conjugate (III) in $200\mu\text{L}$ reaction volume.

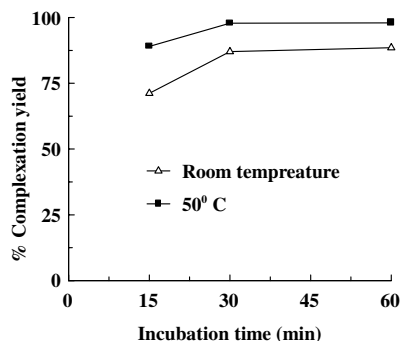


Figure 5. Effect of variation of incubation time and temperature on the complexation yield of the ^{177}Lu labeled sanazole derivative-*p*-amino-DOTA-anilide conjugate (III).

Table 1. Optimum protocol for radiolabeling of sanazole derivative-*p*-amino-DOTA-anilide conjugate (III) with ^{177}Lu

Reagents	Volume/concentration
Sanazole derivative- <i>p</i> -amino-DOTA-anilide conjugate (III)	100 μg (0.14 μM)
0.1 M ammonium acetate buffer, pH ~5	50 μL
Normal saline	125 μL
$^{177}\text{LuCl}_3$ solution (10 $\mu\text{g/mL}$ Lu)	25 μL (~25 MBq)

The reaction mixture was incubated for 30 min at 50°C after adjusting the pH to ~5.

The optimum protocol for complexation as arrived from the above set of experiments is shown in Table 1.

2.6. Purification of ^{177}Lu labeled sanazole derivative-*p*-amino-DOTA-anilide conjugate (III)

The ^{177}Lu labeled conjugate (III) was purified by HPLC using mixtures of acetonitrile and water with 0.1% TFA as the mobile phase. ^{177}Lu labeled sanazole derivative-*p*-amino-DOTA-anilide conjugate (III) exhibited a retention time of 7 min. On the other hand, ^{177}Lu labeled *p*-amino-DOTA-anilide (II) was eluted out in 5.5 min under identical conditions. This experiment provides additional support in favor of the extent of complexation determined by paper chromatography experiments mentioned above. The HPLC patterns of the ^{177}Lu labeled *p*-amino-DOTA-anilide and ^{177}Lu labeled sanazole derivative-*p*-amino-DOTA-anilide conjugate are shown in Figure 6a and b, respectively.

2.7. Stability of ^{177}Lu labeled sanazole derivative-*p*-amino-DOTA-anilide conjugate (III)

The stability of the ^{177}Lu labeled conjugate (III) was studied by employing the standard quality control techniques namely, paper chromatography and HPLC. It was observed that the radiolabeled conjugate retained its radiochemical purity after 7 d of preparation when stored at room temperature.

2.8. Biodistribution studies

To determine the tumor specificity of the ^{177}Lu labeled conjugate (III), the radiolabeled preparation was in-

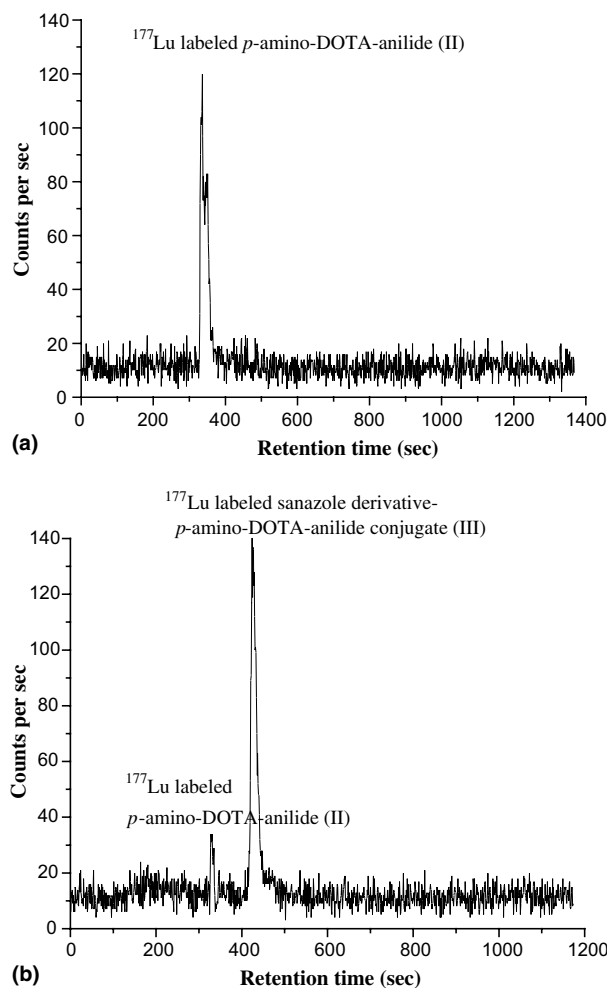


Figure 6. HPLC patterns of (a) ^{177}Lu labeled *p*-amino-DOTA-anilide (II) and (b) ^{177}Lu labeled sanazole derivative-*p*-amino-DOTA-anilide conjugate (III).

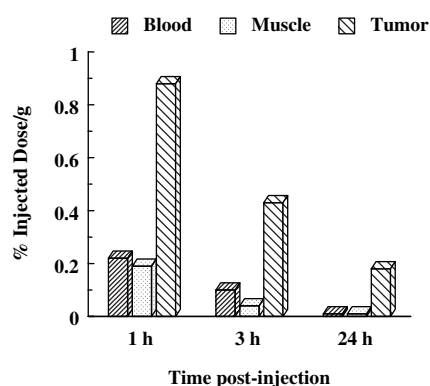
jected in Swiss mice bearing fibrosarcoma tumors. The results of the biodistribution studies are tabulated in Table 2. The biodistribution results show moderate tumor uptake of $0.88 \pm 0.20\%$ of the injected activity per gram within 1 h post-injection. $89.55 \pm 2.32\%$ of the injected activity was observed to clear via the renal route with insignificant accumulation in other major organs/tissues except liver at this time point. Clearance of the activity from all the organs at 24 h post-injection is evident from the $97.69 \pm 0.98\%$ excretion observed at this time point. The activity accumulated in the tumor was also observed to be reduced with progress of time and $0.18 \pm 0.02\%$ of the injected activity per gram was retained in the tumor at 24 h post-injection. However, as the activity cleared out rapidly from all the non-target organs, the tumor to blood and tumor to muscle ratios at all the time points studied were observed to be quite high, which provides additional merit to the potential use of the radiolabeled conjugate for targeted therapy.

Figure 7 depicts the comparative retention of activity in per gram of blood, muscle, and tumor at different post-injection times. It was observed that the tumor to blood ratio was 4.00 and 4.30, respectively, at 1 and 3 h post-

Table 2. Biodistribution pattern of ^{177}Lu labeled sanazole derivative-*p*-amino-DOTA-anilide conjugate (III) in Swiss mice bearing fibrosarcoma tumor

Organ	% Dose/g			
	1 h	3 h	18 h	24 h
Blood	0.22 (0.10)	0.10 (0.04)	0.01 (0.00)	0.01 (0.00)
Liver	1.34 (1.05)	1.34 (0.13)	0.45 (0.10)	0.38 (0.03)
Intestine	0.36 (0.03)	0.26 (0.09)	0.24 (0.09)	0.17 (0.15)
Kidneys	2.76 (0.62)	1.33 (0.31)	0.96 (0.22)	1.01 (0.12)
Stomach	0.30 (0.08)	0.20 (0.10)	0.10 (0.08)	0.06 (0.05)
Heart	0.22 (0.09)	0.04 (0.04)	0.02 (0.02)	0.03 (0.02)
Lungs	0.50 (0.19)	0.13 (0.06)	0.04 (0.02)	0.03 (0.01)
Muscle	0.19 (0.14)	0.04 (0.00)	0.01 (0.00)	0.01 (0.00)
Spleen	0.24 (0.07)	0.09 (0.02)	0.06 (0.00)	0.07 (0.03)
Tumor	0.88 (0.20)	0.43 (0.12)	0.18 (0.03)	0.18 (0.02)
Excretion ^a	89.55 (2.32)	94.77 (1.64)	96.98 (1.27)	97.69 (0.98)

^a%Excretion has been indirectly calculated by subtracting the activity accounted in all the organs from total injected activity.

**Figure 7.** Comparative retention of activity in per gram of blood, muscle, and tumor at different post-injection times.

injection, which gradually increased to 18.00 at 24 h post-injection. On the other hand, tumor to muscle ratio was increased from 4.63 at 1 h post-injection to 10.75 at 3 h post-injection and subsequently reached to 18.00 at

24 h post-injection. It is documented that in case of an ideal tumor-specific agent, the desirable feature sought for, is the localization resulting in target to non-target ratio of greater than 3.0.²³ In the present case, the radiolabeled conjugate exhibited this ratio of 3.0 within 1 h post-injection, which subsequently increased further thereby demonstrating its potential toward use as a hypoxia-avid substrate.

Though hypoxia imaging is a quite well explored field, corresponding therapeutic agents developed with nitroimidazoles, as hypoxia markers are not well documented. Therefore, an attempt to compare the tumor uptake and target to non-target ratios of the radiolabeled conjugate is made with a few standard hypoxia-imaging agents, such as, $^{99\text{m}}\text{Tc}$ -BMS181321²⁴ and $^{99\text{m}}\text{Tc}$ -BRU59-21²⁵ in Table 3. Though not a hypoxia-imaging agent, ^3H -misonidazole,⁵ a genuine label has also been studied as a reference standard. However, it has to be kept in mind that the absolute comparison among the above-mentioned agents are difficult owing to the heterogeneity of animal models used, nature of

Table 3. Comparison of tumor uptake and tumor-to-background ratios of ^{177}Lu labeled sanazole derivative-*p*-amino-DOTA-anilide conjugate (III) with some nitroimidazole based tumor-specific agents

Complex	^3H -misonidazole	$^{99\text{m}}\text{Tc}$ -BMS181321	$^{99\text{m}}\text{Tc}$ -BRU59-21	^{177}Lu labeled III
Tumor	—	$0.73 \pm 0.22^{\text{a}}$	$0.37 \pm 0.04^{\text{a}}$	$0.88 \pm 0.22^{\text{a}}$
	$1.37 \pm 0.45^{\text{b}}$	$0.55 \pm 0.08^{\text{b}}$	$0.37 \pm 0.14^{\text{b}}$	$0.43 \pm 0.12^{\text{c}}$
Blood	—	$3.34 \pm 0.47^{\text{a}}$	$0.53 \pm 0.05^{\text{a}}$	$0.22 \pm 0.10^{\text{a}}$
	$0.73 \pm 0.23^{\text{b}}$	$1.75 \pm 0.27^{\text{b}}$	$0.43 \pm 0.07^{\text{b}}$	$0.10 \pm 0.04^{\text{c}}$
Muscle	—	$0.27 \pm 0.05^{\text{a}}$	$0.11 \pm 0.01^{\text{a}}$	$0.19 \pm 0.14^{\text{a}}$
	$0.89 \pm 0.33^{\text{b}}$	$0.19 \pm 0.05^{\text{b}}$	$0.09 \pm 0.01^{\text{b}}$	$0.04 \pm 0.00^{\text{c}}$
Tumor/blood	—	0.22^{a}	0.70^{a}	4.00^{a}
	1.88^{b}	0.31^{b}	0.86^{b}	4.30^{c}
Tumor/muscle	—	2.72^{a}	3.36^{a}	4.63^{a}
	1.54^{b}	2.89^{b}	4.11^{b}	10.75^{c}
Animal strain	BALB/c mice	C3H mice	C3H/HeJ mice	Swiss mice
Tumor model	KHT-C tumor	KHT-C tumor	KHT-C tumor	Fibrosarcoma
Reference	5	24	25	Present study

^a 1 h Post-injection data.

^b 2 h Post-injection data.

^c 3 h Post-injection data.

the tumors induced and the different post-injection times at which the respective uptakes have been documented. It is evident from Table 3 that ^3H -misonidazole shows highest tumor uptake among all the agents while the tumor uptake exhibited by the remaining three agents are comparable to each other at 2/3 h post-injection. A comparative study, on the other hand shows that the ^{177}Lu labeled conjugate (III) exhibits a superior tumor to blood and tumor to muscle ratios at these time points.

3. Conclusion

Sanazole, a nitroimidazole based hypoxia marker has been successfully coupled with a suitable bifunctional chelating agent, *p*-amino-DOTA-anilide. ^{177}Lu was produced with adequate specific activity and high radionuclidic purity by thermal neutron bombardment using enriched (60.6% ^{176}Lu) Lu_2O_3 target. The coupled product was radiolabeled with ^{177}Lu and the radiolabeled conjugate after purification was used for biodistribution studies in Swiss mice bearing fibrosarcoma tumors. The biodistribution patterns indicate moderate uptake in tumor with high renal clearance along with favorable tumor to blood and tumor to muscle ratios.

4. Experimental

4.1. Materials and methods

Sanazole derivative (I) was obtained as a gift from Radiation Biology and Health Sciences Division of Bhabha Atomic Research Centre. *p*-Amino-DOTA-anilide (II) was procured from M/s. Macrocyclics, USA. Dicyclohexyl carbodiimide (DCC) was obtained from Aldrich Chemical Company, USA. Dioxane was distilled

and dried as per reported procedure.²⁶ All the other chemicals were purchased from reputed local manufacturers and were of analytical grade. Lu_2O_3 (60.6% enriched in ^{176}Lu) powder used as the target for irradiation was procured from M/s. Isoflex, USA.

Radiochemical purity of ^{177}Lu produced was determined by recording γ ray spectra using HPGe detector coupled to a 4K multichannel analyzer (MCA) system. A ^{152}Eu reference source, obtained from Amersham Inc., USA, was used for both energy and efficiency calibration of the detector. All other radioactivity measurements were done using a well-type NaI(Tl) scintillation counter unless otherwise mentioned keeping the base line at 150 keV and window of 100 keV thereby utilizing the 208 keV γ photon of ^{177}Lu .

Flexible silica gel plates IB-F were obtained from Bakerflex Chemical Company, Germany. Whatman 3MM (UK) chromatography paper was used for paper chromatography studies. The high performance liquid chromatography (HPLC) system used was obtained from JASCO, Japan (PU 1580). All the solvents used for HPLC analysis were of HPLC grade and purchased from reputed local manufacturers. The solvents were degassed and filtered prior to use. Fourier transform infrared (FT-IR) spectra were recorded by using Jasco FT/IR-420 spectrophotometer. Proton NMR spectra were recorded on 300 MHz Varian VXR 300S spectrophotometer.

4.2. Coupling of sanazole derivative (I) with *p*-amino-DOTA-anilide (II)

The coupling between sanazole derivative (I) and *p*-amino-DOTA-anilide (II) was achieved by a single-step procedure as depicted in Figure 8. In a typical reaction,

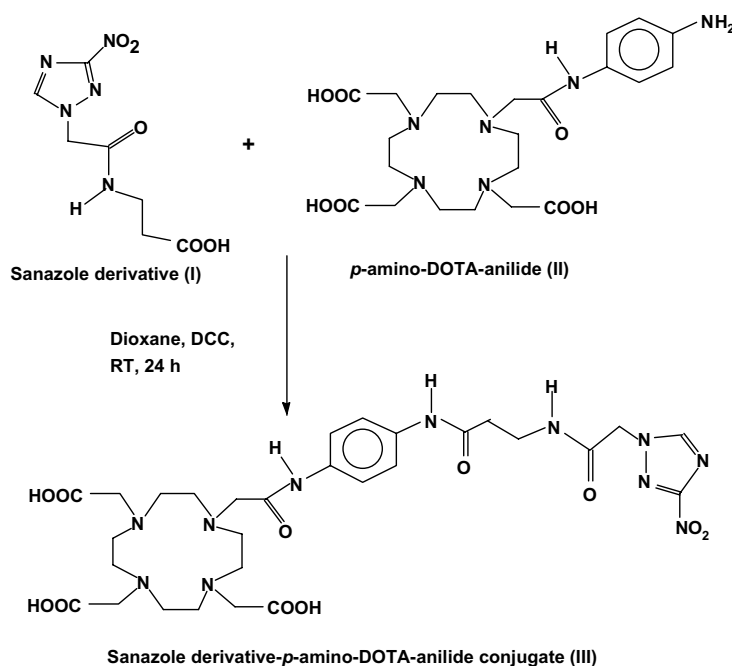


Figure 8. Scheme for coupling of sanazole derivative (I) with *p*-amino-DOTA-anilide (II).

5 mg (0.0205 mM) of sanazole derivative and 13 mg (0.0203 mM) of *p*-amino-DOTA-anilide were dissolved in 2–3 mL of dry dioxane. To this solution, 5 mg (0.0243 mM) of DCC was added and the resulting mixture was stirred at room temperature for a period of 24 h. The progress and completion of the reaction was monitored by thin layer chromatography using 6% ammonium hydroxide in methanol as eluting solvent. After the completion of reaction, the precipitate was separated from the supernatant liquid by filtration and dried. The crude product thus obtained was purified by preparative thin layer chromatography using 2% ammonium hydroxide in methanol as the eluting solvent. The purified conjugate (III) was characterized by FT-IR and ^1H NMR spectroscopy.

4.3. Production of ^{177}Lu

^{177}Lu was produced by thermal neutron bombardment on isotopically enriched (60.6% ^{176}Lu) Lu_2O_3 target at a flux of 3×10^{13} n/cm²/s for 7 d. The target was prepared by evaporating to dryness 20 μL solution (in 0.01 M HCl) of LuCl_3 containing 1 mg/mL of Lu in a quartz ampoule. The ampoule was flame sealed and irradiated after putting it inside an aluminum can. The irradiated target was dissolved in 0.1 M HCl by gentle warming after allowing a cooling period of 6 h. The resulting solution was evaporated to near dryness and reconstituted in doubled distilled water.

The activity of ^{177}Lu produced was assayed by measuring the ionization current by placing an aliquot inside a precalibrated well-type ion chamber. Radionuclidic purity was ascertained by recording the γ ray spectrum of an appropriately diluted $^{177}\text{LuCl}_3$ solution using a HPGe detector coupled to a 4K MCA system. Energy as well as efficiency calibration of the detector were carried out using a standard ^{152}Eu source prior to the assay of activity. Several spectra were recorded for each batch at regular time intervals. Samples measured initially for the assay of ^{177}Lu were preserved for complete decay of ^{177}Lu (over 8–10 half-lives of ^{177}Lu , i.e., for a period of 45–65 d) and re-assayed to determine the activity of long-lived $^{177\text{m}}\text{Lu}$ ($T_{1/2} = 160.5$ d).

4.4. Radiolabeling of *p*-amino-DOTA-anilide (II) with ^{177}Lu

A stock solution of *p*-amino-DOTA-anilide (II) was prepared by dissolving the ligand in 0.1 M ammonium acetate buffer (pH \sim 5) with a concentration of 1 mg/mL. To 50 μL of the stock solution of the ligand, 25 μL of $^{177}\text{LuCl}_3$ (0.25 μg , \sim 25 MBq) was added and the volume of the reaction mixture was made upto 200 μL using normal saline. The reaction mixture was incubated at room temperature for 15 min after adjusting the pH \sim 5.

4.5. Radiolabeling of sanazole derivative-*p*-amino-DOTA-anilide conjugate (III) with ^{177}Lu

For radiolabeling of the sanazole derivative-*p*-amino-DOTA-anilide conjugate (III) with ^{177}Lu , a stock solution of the conjugate was prepared in 0.1 M ammonium

acetate buffer (pH \sim 5) with a concentration of 2 mg/mL. $^{177}\text{LuCl}_3$ (25 μL , 0.25 μg , \sim 25 MBq) was added to 50 μL of the stock solution and the volume of the reaction mixture was made upto 200 μL by addition of normal saline. The pH of the reaction mixture was adjusted to \sim 5 and it was incubated at 50 $^\circ\text{C}$ temperature for 30 min.

Various complexation parameters, such as, ligand concentration, pH of the reaction mixture, reaction time, and temperature were extensively varied in order to achieve the optimum protocol for maximum complexation.

4.6. Quality control techniques

4.6.1. Paper chromatography (PC). Paper chromatography was performed using Whatman 3MM chromatography paper. Portions of the test solutions (5 μL) were applied at 1.5 cm from the lower end of the strip. The strips were developed in suitable solvent, dried, cut into segments of 1 cm each, and the radioactivity was measured.

4.6.2. High performance liquid chromatography (HPLC). HPLC of the ^{177}Lu labeled conjugate was carried out by using a C-18 reversed phase HiQ-Sil (5 μM , 4×250 mm) column. The flow rate was maintained at 1 mL/min. Water (A) and acetonitrile (B) mixtures with 0.1% trifluoroacetic acid (TFA) were used as the mobile phase and the following gradient elution technique was adopted for the separation (0–4 min 95% A, 4–15 min 95% A to 5% A, 15–20 min 5% A, 20–25 min 5% A to 95% A, 25–30 min 95% A). The elution was monitored by detecting radioactivity signal using NaI(Tl) detector.

4.7. Biodistribution studies

Biological behavior of ^{177}Lu labeled conjugate (III) was studied in Swiss mice bearing fibrosarcoma tumors. Fibrosarcoma cells (10^6 cells/mL) in normal saline were prepared and 200 μL was injected into Swiss mice (20–25 g) subcutaneously. The animals were observed for visibility of tumors. At the end of two weeks, tumors of 1 cm diameter were observable. The biodistribution studies were subsequently carried out in the tumor-bearing mice. The complex (\sim 100 μL , \sim 10 MBq activity) was injected through the tail vein. The animals were sacrificed by cardiac puncture post-anesthesia at 1, 3, 18, and 24 h post-injection. Various organs and tumors were excised following sacrifice and the radioactivity associated with each organ/tissue was determined in a flat type NaI(Tl) counter. The percent injected dose (%ID) in various organs/tissues and tumors were calculated from the above data and expressed as percent-injected dose per gram (%ID/g) of organ/tissue. The activity excreted was indirectly determined from the difference between injected dose (ID) and the %ID accounted for in all the organs. To determine the total uptakes in blood, bone, and muscles, it was assumed that 7%, 6.5%, and 40% of the body weight are constituted by blood, bone, and muscles, respectively.²⁷ All the animal experiments were carried out in strict compliance with the relevant

national laws relating to the conduct of animal experimentation.

Acknowledgements

The authors acknowledge the help provided by Dr. S. V. Thakare and Mr. K. C. Jagadeesan for irradiation of Lu target. The authors are also thankful to the staff-members of the Animal House Facility of Bhabha Atomic Research Centre for their sincere help received during animal experimentations. The ^1H NMR spectral facilities rendered by Regional Sophisticated Instrumentation Centre, Indian Institute of Technology, Mumbai is gratefully acknowledged.

References and notes

1. Das, T.; Banerjee, S.; Samuel, G.; Sarma, H. D.; Korde, A.; Venkatesh, M.; Pillai, M. R. A. *Nucl. Med. Biol.* **2003**, *30*, 127.
2. Kapoor, S.; Mathew, R.; Huilgol, N. G.; Kagiya, T. V.; Nair, C. K. K. *J. Radiat. Res.* **2000**, *41*, 355.
3. Nunn, A.; Linder, K.; Strauss, H. W. *Eur. J. Nucl. Med.* **1995**, *22*, 265.
4. Edwards, D. I. *J. Antimicrob. Chemother.* **1993**, *31*, 9.
5. Grunbaum, Z.; Freauff, S. J.; Krohn, K. A.; Wilbur, D. S.; Magee, S.; Rasey, J. S. *J. Nucl. Med.* **1987**, *28*, 68.
6. Chapman, J. D.; Raleigh, J. E.; Pederson, J. E. In *Proceedings of VI International Congress on Radiation Research*; Okada, S., Imamura, M., Terashima, T., Eds.; 1979; pp 885–893.
7. Williams, M.; Jenkins, T. C.; Beveridge, A. J. *J. Chem. Soc., Faraday Trans.* **1996**, *92*, 763.
8. Adams, G. E.; Clarke, E. D.; Flockhart, I. R.; Jacobs, R. S.; Shemi, D. S.; Stratford, I. J.; Wardman, P.; Watts, M. E.; Parrick, J.; Wallace, R. G.; Smithen, C. E. *Int. J. Radiat. Biol.* **1979**, *35*, 133.
9. Adams, G. E.; Clarke, E. D.; Gray, P.; Jacobs, R. S.; Stratford, I. J.; Wardman, P.; Watts, M. E.; Parrick, J. Wallace, R. G.; Smithen, C. E. *Int. J. Radiat. Biol.* **1979**, *35*, 151.
10. Kagiya, V. T. In *Radiobiological Concepts in Radiotherapy*; Bhattacharjee, D., Singh, B. B., Eds.; Narosa Publishing House: New Delhi, 1995; pp 135–146.
11. Shibamoto, Y.; Nishimoto, S.; Mi, F.; Kimura, R.; Sasai, K.; Kagiya, V. T.; Abe, M. *Int. J. Radiat. Biol.* **1987**, *52*, 347.
12. Pillai, M. R. A.; Chakraborty, S.; Das, T.; Venkatesh, M.; Ramamoorthy, N. *Appl. Radiat. Isot.* **2003**, *59*, 109.
13. Smith, C. J.; Gali, H.; Siekman, G. L.; Hayes, D. L.; Owen, N. K.; Mazuru, D. G.; Volkert, W. A.; Hoffman, T. J. *Nucl. Med. Biol.* **2003**, *30*, 101.
14. Stein, R.; Govindan, S. V.; Chen, S.; Reed, L.; Griffiths, J. L.; Hansen, H. J.; Goldenberg, D. M. *J. Nucl. Med.* **2001**, *42*, 967.
15. Das, T.; Chakraborty, S.; Unni, P. R.; Banerjee, S.; Samuel, G.; Sarma, H. D.; Venkatesh, M.; Pillai, M. R. A. *Appl. Radiat. Isot.* **2002**, *57*, 177.
16. Firestone, R. In *Table of Radioisotopes*; Shirley, V. S., Ed.; Wiley: New York, 1996; p 2112.
17. Liu, S.; Edwards, D. S. *Bioconjugate Chem.* **2000**, *12*, 7.
18. Volkert, W. A.; Hoffman, T. J. *Chem. Rev.* **1999**, *99*, 2269.
19. Knapp, F. F.; Ambrose, K. R.; Beets, A. L.; Luo, H.; McPherson, D. W.; Mirzadeh, S. Nuclear Medicine Program Progress Report for Quarter Ending, September 30, 1995; Oak-Ridge National Laboratory, 1995; pp 6–16.
20. Neves, M.; Kling, A.; Lambrecht, R. M. *Appl. Radiat. Isot.* **2002**, *57*, 657.
21. Milenic, D. E.; Garmestani, K.; Chappell, L. L.; Dadachova, E.; Yordanov, A.; Ma, D.; Schlom, J.; Brechbiel, M. W. *Nucl. Med. Biol.* **2002**, *29*, 431.
22. Stimmel, J. B.; Kull, F. C., Jr. *Nucl. Med. Biol.* **1998**, *25*, 117.
23. Strauss, A. W.; Nunn, A.; Linder, K. *J. Nucl. Cardiol.* **1995**, *2*, 437.
24. Ballinger, J. R.; Kee, J. W. M.; Rauth, A. M. *J. Nucl. Med.* **1996**, *37*, 1023.
25. Melo, T.; Duncan, J.; Ballinger, J. R.; Rauth, A. M. *J. Nucl. Med.* **2000**, *41*, 169.
26. Vogel, A. I. *Textbook of Practical Organic Chemistry*, 5th ed.; Longman Scientific Group: London, 1994; p 407.
27. Pillai, M. R. A.; Samuel, G.; Banerjee, S.; Mathew, B.; Sarma, H. D.; Jurisson, S. *Nucl. Med. Biol.* **1999**, *26*, 69.